Contract No:

This document was prepared in conjunction with work accomplished under Contract No. DE-AC09-08SR22470 with the U.S. Department of Energy (DOE) Office of Environmental Management (EM).

Disclaimer:

Proceedings of the ASME 2018 Pressure Vessels and Piping Conference
PVP2018
July 15-20, 2018, Prague, Czech Republic

PVP2018-84334

EFFECT OF HEAT TREATMENT ON THE PROPERTIES OF ADDITIVELY MANUFACTURED TYPE 316L STAINLESS STEEL

Paul S. Korinko
Savannah River National Laboratory
Aiken, SC USA

Michael J. Morgan
Savannah River National Laboratory
Aiken, SC USA

ABSTRACT

Thin wall test articles were made using Fusion Powder Bed processing of Type 316L stainless steel. This hollow structure was fabricated using a Renishaw AM250. The material was characterized in the as fabricated condition using optical, scanning electron microscopy, and tensile testing. The tensile behavior indicates high initial residual stress due to the higher than annealed material yield strength. A series of thermal treatments were investigated to determine the effect on mechanical properties and microstructural evolution. In order to determine these effects, miniature flat tensile test samples and metallographic samples were wire electrical discharge machined from the structure. These samples were vacuum heat treated at 870, 1040 and 1080ºC for 30 to 120 minutes and metallographically examined to determine the microstructural evolution. The samples were tensile tested and the data are evaluated based on the power-law type relationships. AM Type 316L SS exhibits less strain hardening than wrought stainless steel. In addition, the ductility is somewhat lower in the as-fabricated condition compared to the heat-treated condition. The results of the testing and the rationale for these different behaviors will be discussed.

INTRODUCTION

Additive Manufacturing (AM), the fabrication of components in a layer by layer manner using from a computer aided design (CAD) file that is parsed into processing layers and solidified using powder feedstock and a heat source, is becoming a mainstream approach to fabricate high value components that are difficult to produce using conventional means (1-4). For instance, General Electric is using AM to fabricate fuel nozzles that were comprised of dozens of parts joined together and now can be fabricated directly. AM can be accomplished using several different approaches and heat sources. These include Laser Powder Bed Fusion (L-PBF), electron beam powder bed fusion (EB-PBF) and directed energy powder or wire processes. The process chosen will depend on a variety of factors that include the required fidelity of the part, the requisite surface condition, the desired properties, the availability of feedstock, etc. (5). L-PBF processing conditions have primarily been developed for titanium, aluminum and stainless steels.

Austenitic stainless-steel (SS) alloys, like Type 316L SS, are good candidates for AM since they have well behaved solidification modes, are routinely laser welded and have well defined processing parameters (6-8). AM can generate internal defects, however, from providing insufficient energy to melt and fuse the layers resulting in lack of fusion defects, or keyhole defects from excessive energy density and rapid cooling rates trapping porosity within the structure. Despite the possibility of producing these defects, 316L SS is widely used to fabricate AM components and test articles. In fact, L-PBF has been proposed to fabricate heat exchanger tubing. The materials, both actual and surrogate have been studied extensively at Savannah River National Laboratory (9-11). The efforts to date have been on the optimization and characterization of the stainless steel in the as-fabricated condition. Although there is interest in stress relief heat treatments and hot isostatic pressing to achieve full density.

As-fabricated austenitic SS when processed by L-PBF often-times exhibit dislocation structures that are suggestive of significant levels of cold work. These dislocations are caused by the rapid cooling and levels of constraint during solidification and cooling. The dislocation tangles and loops and density of dislocations manifest themselves in the relatively high yield strength, compared to annealed wrought SS, of as-fabricated materials. The appearance of cold work type defects is also observed in the lower elongation to failure measured in some AM materials (12-14).

LB-PBF AM results in significant levels of residual stress. The effect of the residual stress can result in lower ductility and potentially lower fracture toughness. This study was undertaken to understand the effects of heat treatment on the tensile properties of L-PBF processed Type 316L SS. Samples were removed from surrogate materials that were prepared as part of the fabrication of a coil component. Samples were heat treated at a subcritical annealing temperature to annealing temperatures and the properties are compared to the properties of wrought Type 316L SS. The details of the results are discussed.

NOMENCLATURE

AM	Additive Manufacturing
d	Displacement
ε	Strain
EDM	Electric Discharge Machining
F	Force
HT	Heat Treat
L-PBF	Laser Powder Bed Fusion
OM	Optical Microscope
σ	Stress
SEM	Scanning Electron Microscope
SRNL	Savannah River National Laboratory
SS	Stainless Steel
X	Magnifications

EXPERIMENTAL

A Renishaw AM250 at the Oak Ridge National Laboratory's Manufacturing Development Facility (ORNL MDF) was used to fabricate these samples. These samples were cut from excess materials that were fabricated simply as supports for powder grab samples, as shown in Figure 1. The conditions used to fabricate the total build, which include the actual component in addition to the square tubes are listed in Table 1. Note that contrary to good processing, there were no contour passes around the external surface. This absence leads to a rough surface. Samples were extracted from near the center of the square pipe tube using electrical discharge machining (EDM).

Sub-sized tensile and metallography samples perpendicular and parallel to the were wire EDM from the center section of a 150 mm long square pipe. The geometry of the tensile samples is shown in Figure 2.

Tensile and metallography samples were vacuum heat treated after heating the empty vacuum furnace to 1200°C. Samples were heat treated at 870, 1040, and 1080°C for 30, 60, and 120 minutes. To prevent deformation, due to residual stress, during heating flat stainless steel (SS) weights were placed on the samples. The samples were heated at a rate of 10°C./min to the target temperature and furnace cooled to less than 300°C and then argon gas cooled.

Tensile testing was conducted using an MTS Criterion. A 5 mm extensometer, 10000 kN load cell, and a 0.005 / min strain rate were used. The yield stress, modulus, and UTS were determined using the MTS software.

Fractured samples were examined using an Hitachi X850 Scanning Electron Microscope at an accelerating voltage of 20kV at magnifications from 20 to 30,000X.

Metallographic samples were cut parallel and perpendicular to the print direction, mounted in epoxy, ground, polished, and electrolytically etched with 10% oxalic acid for 30 to 120 seconds and examined using an optical microscope. Images were taken at 50 to 500X magnifications. The microstructures were compared to the as-fabricated condition.

RESULTS AND DISCUSSION

Figure 3 shows the samples as they were cut from the center of the square tubes. Note that they are parallel to the fabrication direction. The metallographic samples were taken from these remnants.

The as-received microstructures both parallel and perpendicular to the build direction are shown in Fig. 4. The as-received microstructure parallel to the build direction, Figs. 4a-c exhibits a "fish scale" structure due to the melt pool solidification in the vertical orientation. Periodic horizontal lines are visible at low magnification, Fig. 4a, where the Renishaw controls software changes the melt pattern. The grains and melt lines are visible and the grains appear to extend across the melt pool lines, Figs. 4b and 4c. The presence of isolated porosity is evident in these images at high magnification. The microstructure perpendicular to the build direction is shown in Figs 4d-4f. It exhibits the "basket weave" microstructure, clearly shown in Fig. 4d at low magnification, associated with the scanning pattern typically used for L-BPF. Evidence of the melt pool is visible in Fig. 4e. Randomly oriented grains are apparent at high magnification in Fig. 4f. The sample also some tiny porosity.

The samples were heat as indicated above and were examined metallographically. All of the samples exhibited microstructural evolution during the heat treatment with some conditions more clearly causing changes. The microstructure evolution for each temperature is shown in Figures 6-8. These images indicate that recrystallization has occurred and the grains are growing. In addition, the evidence of the prior melt boundaries are eliminated. This feature can be seen at temperatures as low as 870°C for 30 minutes, Figure 6a. The presence of the melt interfaces is not observed at all for the 1040°C / 30 minute exposure. 870°C is considered below the heat treatment temperature of the 300 series stainless steels.

An attempt to measure grain growth for each of the exposure conditions was made; these results are not conclusive since the microstructure is complex and the presence of the grain boundaries is not obvious in many of the micrographs, but a typical grain boundary is shown by the arrows. The results are presented in Table 2. The standard deviations are listed and are fairly large. However, there is some correlation of increased grain size with increased time and temperature, as expected.

The tensile properties of a forged Type 304L stainless steel were tested as part of another project; the results for a typical orientation of this material are shown in Figure 8 for reference. This material exhibits a fairly low strain hardening curve which is consistent with the amount of cold work associated with the forging process and yield strength. The material exhibits tensile elongations that are greater than 50%.

The tensile curves for the AM type 316L SS in the as-fabricated condition is shown in Figure 9. These samples also exhibit a low hardening exponent. As a simple method to compare the hardening exponents, the ratio of the UTS to the YS was calculated. Using this value, it is apparent that the baseline (BL) sample has the lowest effective hardening. This result is likely due to the extensive dislocation network and relatively high residual stresses present in SLM produced AM structures (16,17).

The tensile properties after the 870°C heat treatment exhibit varying results as shown in Fig.10. There was a significant increase in the yield strength of one of the samples with an increase in the ratio of UTS to YS (hardening factor) in all of the samples compared to the baseline. It is surmised that the increased yield strength is associated with changes to the grain size of the individual samples, although metallographic examination of the associated samples was inconclusive.

Figure 11 shows the tensile curves after the 1040°C heat treatment. All the samples exhibit similar yield and tensile strengths. The relative hardening factors are also similar for these samples. This temperature is consistent with the suggested annealing temperature so the significant reduction in yield strength results are consistent with what is expected for traditionally produced Type 304L materials as indicated in Table 2, annealed bar (B) and plate (P), however, the UTS and ductility are lower. Since the samples were cut from as fabricated material, and there are both pores and some surface defects, the UTS and elongation may be adversely affected by these conditions. Other researchers have shown that internal defects and build defects adversely affect ductility measurement.

Figure 12 compares the tensile properties of the samples heat treated for 2 hours at the three temperatures. These data indicate a modest decrease in yield strength with increasing temperature which may ultimately be attributable to grain size effects if additional characterization is conducted. The slight increase in elongation with temperature may be due to the reduced dislocation density or the random nature of porosity in these materials. Further these effects may be potentially convoluted with surface effects and random porosity in the samples.

Figure 13 shows the summary tensile strength data for AM, forged and comparison data. These results clearly indicate that the YS of AM and annealed AM thin blades lie within the nominal properties while the UTS is somewhat lower than expected (7, 18 & 19). Again, lower UTS may be attributed to the presence of the defects that cause lower ductility. The summary data are presented in Table 3.

CONCLUSIONS

Simple heat treating of SLM AM Type 316 L SS does not affect the internal defects formed during additive manufacturing. Heat treatment reduces the yield strength of the material as dislocations and other strengthening mechanisms for austenitic SS are removed from the microstructure. The ultimate tensile strength is moderately affected. The elongation properties of AM materials are dominated by the residual porosity and by the surface conditions.

Heat treatment can be used to decrease the yield strength, but it has less effect on the elongation since the defect structure dominates. Other measures of ductility, reduction in area, for instance, may provide a more complete measurement of the effects of heat treatment as well as the defects on AM materials.

Full annealing is accomplished under conditions that are similar to those used for conventional materials, i.e., 1040°C for 2 hours.

ACKNOWLEDGMENTS

This document was prepared for the U.S. Department of Energy under contract number DE-AC09-08SR22470. The authors would like to acknowledge the assistance of F. List, III, K. Carver, and S. Babu of Oak Ridge National Laboratory's Manufacturing Development Facility for sample fabrication and processing. They would also like to recognize M. Van Swol, A. Hollingshad, D. Thompson, and K. Imrich of the Savannah River National Laboratory for their assistance in sample preparation and examination, heat treatment, and sample cutting. Finally, they would like to recognize S. Wyrick for program management and financial support.

REFERENCES

1. Lawrence E. Murr, Sara M. Gaytan, Diana A. Ramirez, Edwin Martinez,Jennifer Hernandez, Krista N. Amato, Patrick W. Shindo, Francisco R. Medina1, and Ryan B. Wicker, "Metal Fabrication by Additive Manufacturing Using Laser and Electron Beam Melting Technologies", J. Mater. Sci. Technol., 2012, 28(1), 1–14.

2. Kaufui V.Wong and Aldo Hernandez, "A Review of Additive Manufacturing", International Scholarly Research Network, ISRN Mechanical Engineering, Volume 2012, Article ID 208760.

3. S. S. Babu and R. Goodridge, "Additive Manufacturing", Materials Science and Technology 2015 VOL 31 NO 8.

4. D D Gu, W Meiners, K Wissenbach & R Poprawe, "Laser Additive Manufacturing Of Metallic Components: Materials, Processes And Mechanisms", International Materials Reviews, 57:3, 133-164 2012.

5. B. Vayrea,, F. Vignata, F. Villeneuvea, "Designing for Additive Manufacturing", 45th CIRP Conference on Manufacturing Systems 2012, Procedia CIRP 3 (2012) 632 – 637.

6. G. Miranda, S. Faria, F. Bartolomeu, E. Pinto, S. Madeira, A. Mateus, P. Carreira, N. Alves, F.S. Silva, O.

Carvalho, Predictive Models for Physical and Mechanical Properties Of 316L Stainless Steel Produced By Selective Laser Melting, Materials Science & Engineering A 657 (2016) 43 – 56.

7. Kurian Antony, N. Arivazhagan, K. Senthilkumaran, Numerical and Experimental Investigations on Laser Melting of Stainless Steel 316L Metal Powders, Journal of Manufacturing Processes 16 (2014) 345–355.

8. Wes Everhart, Paul Korinko, Marissa Reigel, Michael Morgan, and John Bobbitt, CHARACTERIZATION OF SELECTIVE LASER MELTED 304L, Published in the Proceedings of MS&T 16, Materials Science and Technology, Salt Lake City, UT, Oct. 23-27, 2016

9. Paul Korinko, John Bobbitt, Haley McKee,Frederick List, III and J.K. Carver, CHARACTERIZATION OF ADDTIVELY MANUFACTURED HEAT EXCHANGER TUBING, published in A SME 2017 Pressure Vessels and Piping Conference, PVP2017, July 16-20, 2017, Waikoloa, Hawaii, United States

10. Paul Korinko, John Bobbitt, Haley McKee,Frederick List, III and S. S. Babu, OPTIMIZING, FABRICATING AND CHARACTERIZING ADDTIVELY MANUFACTURED HEAT EXCHANGER TUBING, Published in Proceedings of TMS 2017 146th ANNUAL MEETING & EXHIBITION, February 26-March 2, 2017 • San Diego, CA, USA

11. Paul Korinko, John Bobbitt, Michael Morgan, Marissa Reigel, Frederick List, III and S. Suresh Babu, CHARACTERIZATION OF ADDITIVE MANUFACTURING FOR PROCESS TUBING, Submitted for publication in Additive Manufacturing, Nov. 2017

12. Jyoti Suryawanshi, K.G. Prashanth, U. Ramamurty, Mechanical Behavior Of Selective Laser Melted 316L Stainless Steel,Materials Science & Engineering A, 696, 2017, 113-121.

13. R. Casati, J. Lemke, M. Vedani, Microstructure and Fracture Behavior of 316L Austenitic Stainless Steel Produced by Selective Laser Melting, Journal of Materials Science & Technology 32 (2016) 738–744.

14. Baicheng Zhang · Lucas Dembinski · Christian Coddet, The study of the laser parameters and environment variables effect on mechanical properties of high compact parts elaborated by selective laser melting 316L powder, Materials Science and Engineering A, 584 (2013) 21-31.

15. Zhongji Sun, Xipeng Tan, Shu Beng Tor, Wai Yee Yeong, Selective Laser Melting of Stainless Steel 316L With Low Porosity and High Build Rates, Materials and Design 104 (2016) 197- 204.

16. D.W. Brown, J.D. Bernardin, J.S. Carpenter, B. Clausen, D. Thompson, Neutron Diffraction Measurements of Residual Stress in Additively Manufactured Stainless Steel, Materials Science & Engineering A, 678, (2106) 291-298.

17. Xiaohui Chen, Jia Li, Xu Cheng, Huaming Wang, Zheng Huang, Effect of heat treatment on microstructure, mechanical and corrosion properties of austenitic stainless steel 316L using arc additive manufacturing, Materials Science & Engineering A

18. http://www.matweb.com/search/DataSheet.aspx?MatGUID=072da6c8d36c4c519a87c9b082c58cd3&ckck=1, 304 Stainless Steel (UNS S30400); Annealed Bar, Feb. 14, 2018

19. http://www.matweb.com/search/DataSheet.aspx?MatGUID=ec1666b2959f4746906341d6d91cfd29, 304 Stainless Steel (UNS S30400); Annealed Plate, Feb. 14, 2018

TABLE 1. FABRICATION PARAMETERS FOR THE SAMPLE BUILD.

Parameter	Renishaw 316L SS Build 4
Powder size	15-45µm
Laser Power used	**120 W**
Layer thickness	50 µm
Scan Pattern	Stripe—5 mm
Beam Size	75 µm
Point distance	60 µm
Point exposure	80 µs
Effective Velocity	0.64 m/s
Hatch Spacing	**100 µm**
Volume Power	200 W

TABLE 2. MEASURED GRAIN SIZES OF THE SAMPLES AFTER HEAT TREATMENT.

Condition	Grain Size (µm)	Standard Dev.
BL		
870°C/120 m	26	4.4
1040°C/120 m	31	5.2
1080°C/120 m	33	6.0

TABLE 3. TENSILE AND COMPARISON DATA FOR THE AM AND FORGED MATERIALS COMPARED TO THE STANDARDS (18 & 19)

	YS	UTS	Ef	UTS/YS
Forged	477	703	0.5	1.47
BL	390	506	0.23	1.30
870/30	417	643	0.28	1.54
870/60	344	521	0.33	1.51
870/120	333	503	0.22	1.51
1040/30	313	498	0.30	1.59
1040/60	304	501	0.35	1.65
1040/120	299	484	0.27	1.62
1080/120	282	476	0.32	1.69
Annealed B	235	640	0.76	2.72
Annealed P	330	590	0.64	1.79

FIG. 1. SPECIMEN COIL, FABRICATED FOR OTHER TESTING, AND TOWER, INDICATED BY ARROW, WHICH WAS USED FOR HEAT TREATMENT STUDIES.

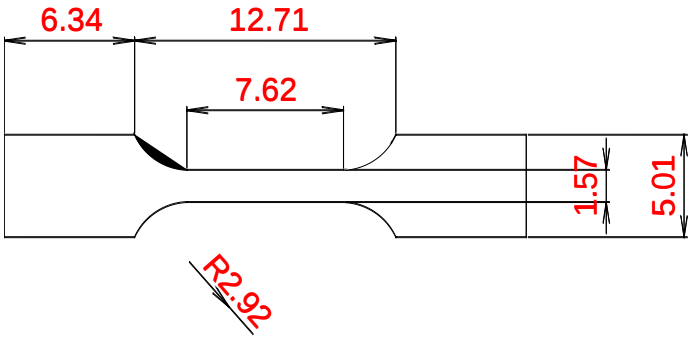

FIG. 2. DIMENSIONS OF THE MINI-TENSILE SAMPLES THAT WERE WIRE EDM FROM THE TOWERS. THE THICKNESS OF THE SAMPLES WAS NOMINALLY 0.7 mm.

FIG. 3. APPEARANCE OF THE SQUARE TUBE AFTER MINI-TENSILES WERE MACHINED.

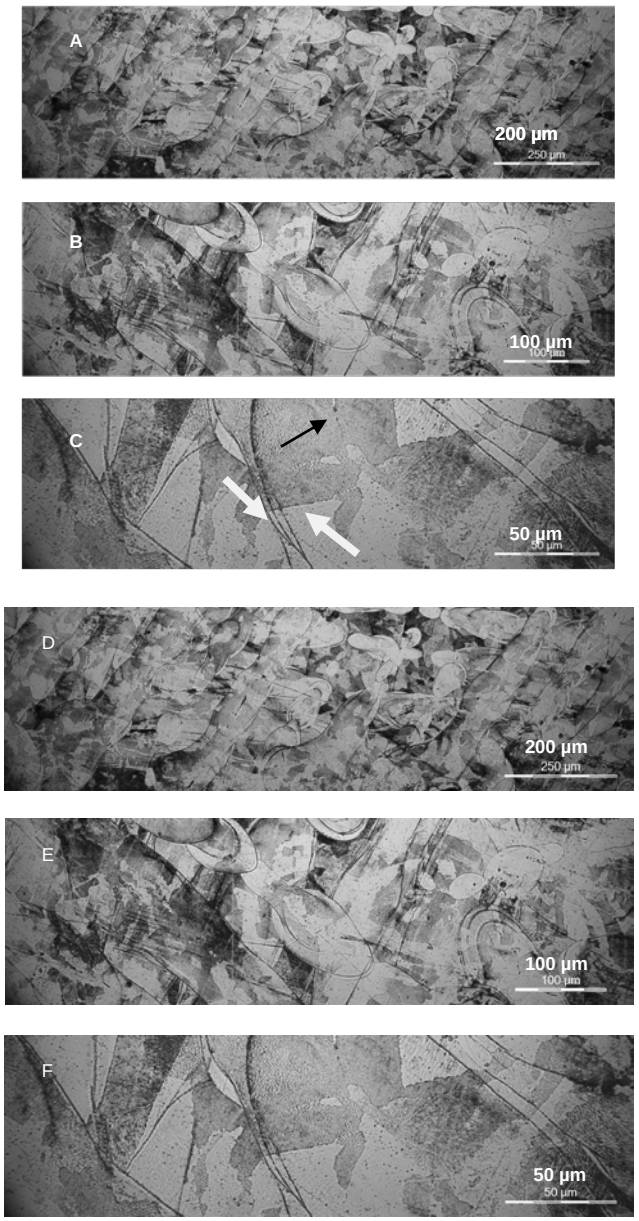

FIG. 4. AS-FABRICATED TYPE 316L SS SHOWN PARALLEL (A-C) AND PERPENDICULAR (D-F) TO THE BUILD DIRECTION; A) LOW MAGNIFICATION, B) MODERATE MAGNIFICATION, C) HIGH MAGNIFICATION. SHOWN PERPENDICULAR TO THE BUILD DIRECTION; A) LOW MAGNIFICATION, B) MODERATE MAGNIFICATION, C) HIGH MAGNIFICATION. D) LOW MAGNIFICATION, E) MODERATE MAGNIFICATION, F) HIGH MAGNIFICATION. NOTE GRAINS EXTENDING ACROSS LASER MELT LINES, AT WHITE ARROWS IN (C). NOTE SMALL PORES AT BLACK ARROW IN (C),

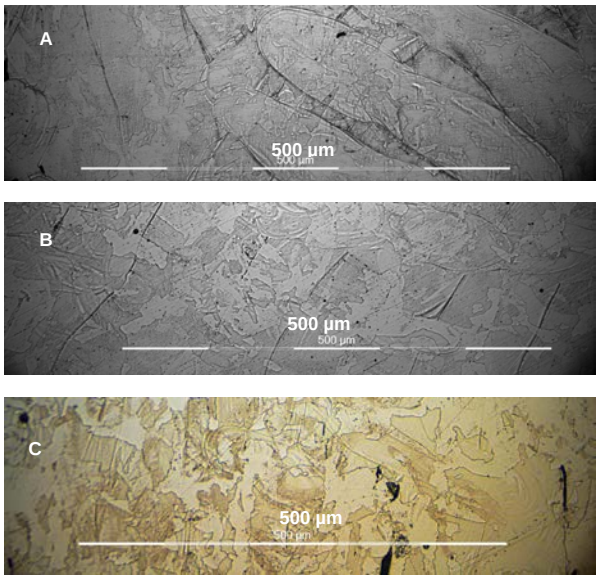

FIG. 5. MICROSTRUCTURE OF AM TYPE 304L SS PERPENDICULAR TO THE BUILD DIRECTION AFTER HEAT TREATING AT 870ºC FOR (A) 30 MINUTES (60) MINUTES AND (C) 120 MINUTES.

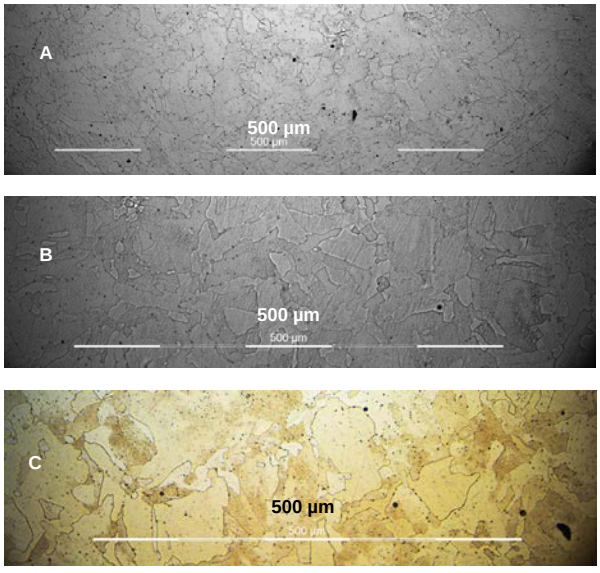

FIG. 6. MICROSTRUCTURES OF AM TYPE 316L SS PERPENDICULAR TO THE BUILD DIRECTION AFTER HEAT TREATING AT 1040ºC FOR (A) 30 MINUTES (60) MINUTES AND (C) 120 MINUTES. NOTE THAT THE LASER MELT POOL LINES HAVE BEEN ELIMINATED, SEE FIGURE FIG. 4E FOR COMPARISON.

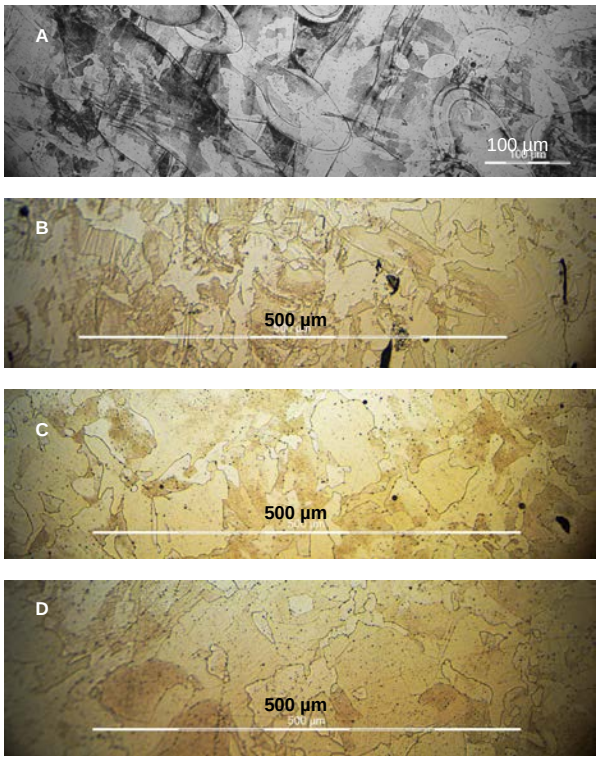

FIG. 7. MICROSTRUCTURE OF AM TYPE 304L SS AFTER HEATING TREATING FOR 120 MINUTES AT (A) AS FABRICATED (B) 870^{O}C (C) 1040^{O}C AND (D) 1080^{O}C.

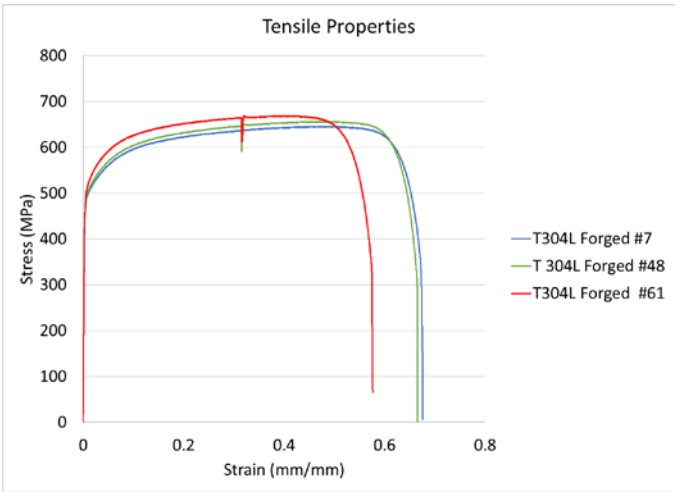

FIG. 8. TENSILE PROPERTIES OF FORGED TYPE 304l STAINLESS STEEL, PARALLEL TO FORGING

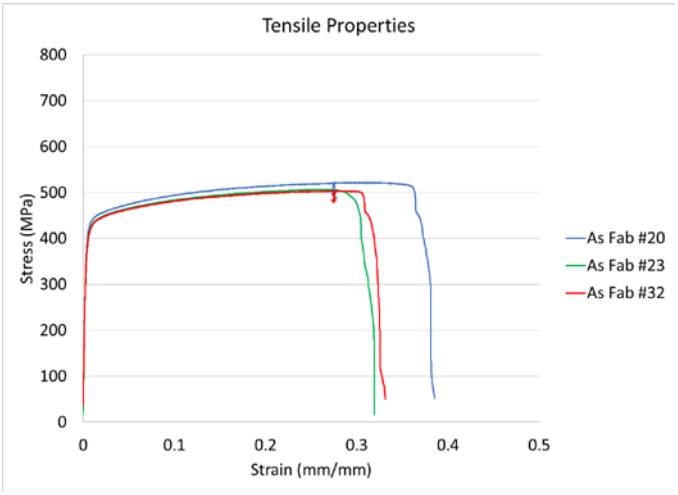

FIG. 9. TENSILE PROPERTIES OF AM TYPE 304L SS IN THE AS-FABRICATED CONDITION.

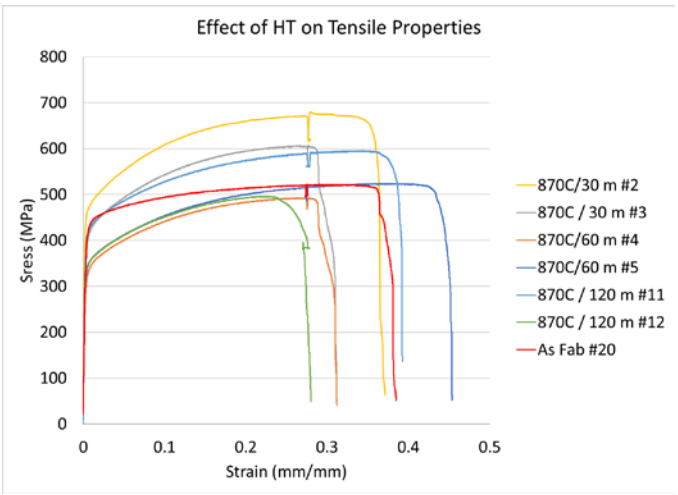

Fig. 10. TENSILE DATA FOR THE SAMPLES HEAT TREATED AT 870^{O}C FOR 30 TO 120 MINUTES COMPARED TO A TYPICAL AS FABRICATED SAMPLE (RED CURVE).

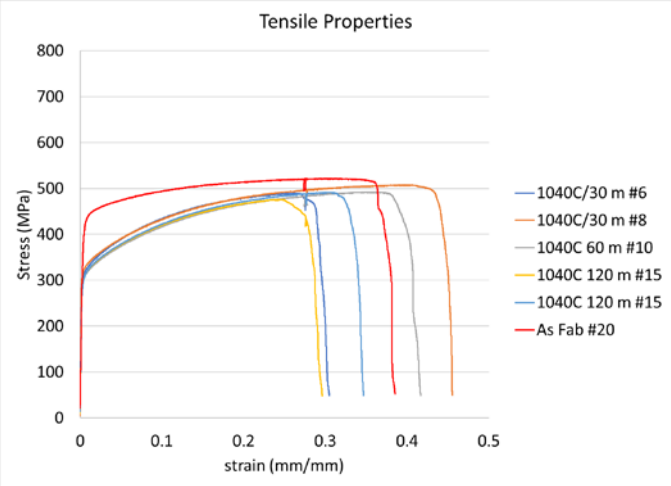

Fig. 11. TENSILE DATA FOR THE SAMPLES HEAT TREATED AT 1040^{O}C FOR 30 TO 120 MINUTES COMPARED TO A TYPICAL AS FABRICATED SAMPLE (RED CURVE).

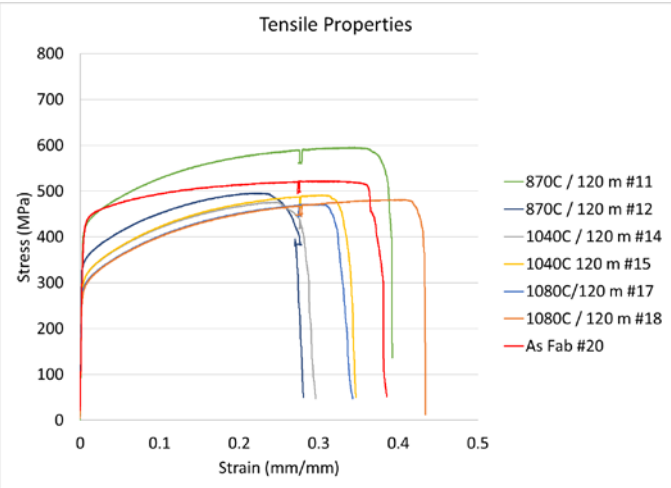

Fig. 12. TENSILE DATA FOR THE SAMPLES HEAT TREATED AT 870^{O}C, 1040^{O}C, AND 1080^{O}C FOR 120 MINUTES COMPARED TO A TYPICAL AS FABRICATED SAMPLE (RED CURVE).

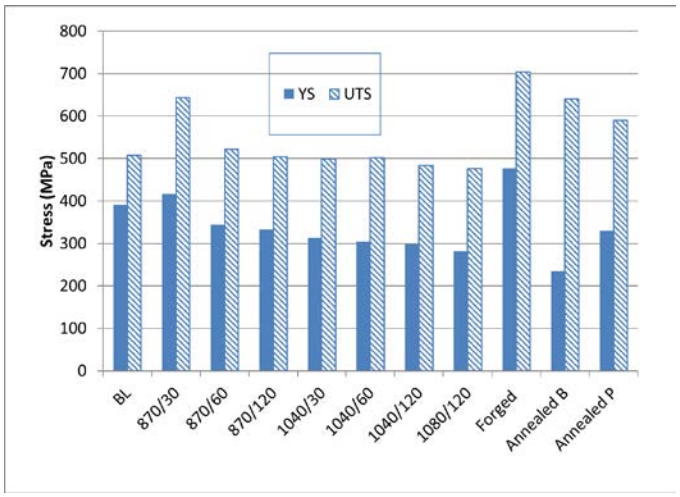

FIG. 13. A COMPARISON OF THE YIELD AND TENSILE PROPERTIES OF AS-FABRICATED AND HEAT TREATED AM TYPE 316L SS COMPARED TO FORGED TYPE 304L AND ANNEALED PROPERTIES (18,19).